

Consistent analysis of the $B \rightarrow \pi$ transition form factor in the whole physical regionTao Huang^{1,2,*} and Xing-Gang Wu^{2,†}¹*CCAST (World Laboratory), P.O. Box 8730, Beijing 100080, China*²*Institute of High Energy Physics, Chinese Academy of Sciences, P.O. Box 918(4), Beijing 100049, China*

(Received 30 December 2004; published 22 February 2005)

In this paper, we show that the $B \rightarrow \pi$ transition form factor can be calculated by using the different approach in the different q^2 regions and they are consistent with each other in the whole physical region. For the $B \rightarrow \pi$ transition form factor in the large recoil regions, one can apply the perturbative quantum chromodynamics (PQCD) approach, where the transverse momentum dependence for both the hard-scattering part and the nonperturbative wave function, the Sudakov effects and the threshold effects are included to regulate the endpoint singularity and to derive a more reliable PQCD result. Pionic twist-3 contributions are carefully studied with a better endpoint behavior wave function for Ψ_p and we find that its contribution is less than the leading twist contribution. Both the two wave functions Ψ_B and $\bar{\Psi}_B$ of the B meson can give sizable contributions to the $B \rightarrow \pi$ transition form factor and should be kept for a better understanding of the B decays. The present obtained PQCD results can match with both the QCD light cone sum rule results and the extrapolated lattice QCD results in the large recoil regions.

DOI: 10.1103/PhysRevD.71.034018

PACS numbers: 12.38.Aw, 12.38.Bx, 13.20.He

I. INTRODUCTION

There are various approaches to calculate the $B \rightarrow \pi$ transition form factor, such as the lattice QCD technique [1–3], the QCD light cone sum rules (LCSRs) [4–7], and the perturbative QCD (PQCD) approach [8–13]. The PQCD calculation is reliable only when the involved energy scale is hard enough, i.e., in the large recoil regions. Because of the restriction to the π energies smaller than the inverse lattice spacing, the lattice QCD calculation becomes more difficult in the large recoil regions and at present, the lattice QCD results of the $B \rightarrow \pi$ transition form factor are available only for soft regions, i.e., $q^2 > 15 \text{ GeV}^2$. The lattice QCD results can be extrapolated to small q^2 regions, and the different extrapolation methods might cause uncertainties of about 5% [2]. Meanwhile, the QCD LCSRs can involve both the hard and the soft contributions below $q^2 < 18 \text{ GeV}^2$ [4] and can be extrapolated to higher q^2 regions [5–7]. Therefore, the results from the PQCD approach, the lattice QCD approach, and the QCD LCSRs are complementary to each other, and by combining the results from these three methods, one may obtain a full understanding of the $B \rightarrow \pi$ transition form factor in its physical region, $0 \leq q^2 \leq (M_B - M_\pi)^2 \simeq 25 \text{ GeV}^2$.

Certain exclusive processes involving hadrons can be described by PQCD if the momentum transfer is sufficiently large. The amplitude can be factorized into the convolution of the nonperturbative wave function for each of the hadrons with a PQCD calculable hard-scattering amplitude. The PQCD factorization theorem has been worked out in Refs. [14,15] based on the earlier works on the applications of PQCD to hard exclusive processes [16]. In the present paper, we shall use the

PQCD approach to calculate the $B \rightarrow \pi$ transition form factor in the large recoil regions.

In the PQCD approach based on the collinear factorization theorem, a direct calculation of the one-gluon-exchange diagram for the B meson transition form factor suffers singularities from the endpoint region of a momentum fraction $x \rightarrow 0$. Because of these singularities, it was claimed that the $B \rightarrow \pi$ transition form factor is dominated by soft dynamics and not calculable in PQCD [17]. In fact, in the endpoint region the parton transverse momenta \mathbf{k}_\perp are not negligible. After including the parton transverse momenta, large double logarithmic corrections $\alpha_s \ln^2 k_\perp$ appear in higher order radiative corrections and must be summed to all orders. In addition, there are also large logarithms $\alpha_s \ln^2 x$ which should also be summed (threshold resummation [18]). The relevant Sudakov form factors from both k_\perp and the threshold resummation can cure the endpoint singularity which makes the calculation of the hard amplitudes infrared safe, and then the main contribution comes from the perturbative regions.

An important issue for calculating the $B \rightarrow \pi$ transition form factor is whether we need to take both wave functions Ψ_B and $\bar{\Psi}_B$ into consideration or simply Ψ_B is enough? In literature, many authors (see Refs. [9–11]) did the phenomenological analysis with only Ψ_B , setting $\bar{\Psi}_B = 0$ (or strictly speaking, ignoring the contributions from $\bar{\Psi}_B$). However, as has been argued in Refs. [19,20], one may observe that the distribution amplitudes (DAs) of those two wave functions have a quite different endpoint behavior, such a difference may be strongly enhanced by the hard-scattering kernel. Even though $\bar{\Psi}_B$ (with the definition in Ref. [13]) is of subleading order contribution, there is no convincing motivation for setting $\bar{\Psi}_B = 0$. In the present paper, we shall keep both wave functions Ψ_B and $\bar{\Psi}_B$ to do our calculations and show to what extent the $\bar{\Psi}_B$ can affect

*Email: huangtao@mail.ihep.ac.cn

†Email: wuxg@mail.ihep.ac.cn

the final results. Another issue we need to be more careful about is about the pionic twist-3 contributions. Based on the asymptotic behavior of the twist-3 DAs, especially $\phi_p^{as}(x) \equiv 1$, most of the people pointed out a large twist-3 contribution [12,21] to the $B \rightarrow \pi$ transition form factor, i.e., bigger than that of the leading twist in almost all of the energy regions. In Ref. [22], the authors have made a detailed analysis on the model dependence of the twist-3 contributions to the pion electromagnetic form factor, and have raised a new twist-3 wave function with a better endpoint behavior for Ψ_p , which is derived from the QCD sum rule moment calculation [23]. Their results show that with the new form for Ψ_p , the twist-3 contributions to the pion electromagnetic form factor are power suppressed in comparison to the leading twist contributions. According to the power counting rules in Ref. [21], the pionic twist-2 and twist-3 contributions should be of the same order for the case of the B meson decays. With the new form for Ψ_p [22], we show that for the case of the $B \rightarrow \pi$ transition form factor, even though the twist-3 contributions are of the same order of the leading twist contributions, its values are less than the leading twist contribution.

The purpose of the paper is to examine the $B \rightarrow \pi$ transition form factor in the PQCD approach, and to show how the PQCD results can match with the QCD LCSR results and the extrapolated lattice QCD results. In the PQCD approach, the full transverse momentum dependence (k_T -dependence) for both the hard-scattering part and the nonperturbative wave function, the Sudakov effects and the threshold effects are included to cure the endpoint singularity. In Sec. II, based on the k_T factorization formalism, we give the PQCD formulae for the $B \rightarrow \pi$ transition form factor in the large recoil regions. In Sec. III, we give our numerical results and carefully study the contributions from Ψ_B and $\bar{\Psi}_B$, and those from the different pionic twist structures. The slope of the obtained form factors $F_{+0}^{B\pi}(q^2)$ in the large recoil regions can match with those obtained from other approaches. Conclusion and a brief summary are presented in the final section.

II. $B \rightarrow \pi$ TRANSITION FORM FACTOR IN THE LARGE RECOIL REGIONS

First, we give our convention on the kinematics. For convenience, all the momenta are described in terms of the light cone (LC) variables. In the LC coordinate, the momentum is described in the form, $k = (\frac{k^+}{\sqrt{2}}, \frac{k^-}{\sqrt{2}}, \mathbf{k}_\perp)$, with $k^\pm = k^0 \pm k^3$ and $\mathbf{k}_\perp = (k^1, k^2)$. The scalar product of two arbitrary vectors A and B is, $A \cdot B = \frac{A^+ B^- + A^- B^+}{2} - \mathbf{A}_\perp \cdot \mathbf{B}_\perp$. The pion mass is neglected and its momentum is chosen to be in the minus direction. Under the above convention, we have $P_B = \frac{M_B}{\sqrt{2}}(1, 1, \mathbf{0}_\perp)$, $P_\pi = \frac{M_B}{\sqrt{2}} \times (0, \eta, \mathbf{0}_\perp)$, and $\bar{P}_\pi = \frac{M_B}{\sqrt{2}}(\eta, 0, \mathbf{0}_\perp)$, with $\eta = 1 - \frac{q^2}{M_B^2}$ and $q = P_B - P_\pi$.

The two $B \rightarrow \pi$ transition form factors $F_+^{B\pi}(q^2)$ and $F_0^{B\pi}(q^2)$ are defined as follows:

$$\langle \pi(P_\pi) | \bar{u} \gamma_\mu b | \bar{B}(P_B) \rangle = \left[(P_B + P_\pi)_\mu - \frac{M_B^2 - m_\pi^2}{q^2} q_\mu \right] \times F_+^{B\pi}(q^2) + \frac{M_B^2 - m_\pi^2}{q^2} q_\mu F_0^{B\pi}(q^2), \quad (1)$$

where $F_+^{B\pi}(0)$ should be equal to $F_0^{B\pi}(0)$ so as to cancel the poles at $q^2 = 0$.

The amplitude for the $B \rightarrow \pi$ transition form factor can be factorized into the convolution of the wave functions for the respective hadrons with the hard-scattering amplitude. The wave functions are nonperturbative and universal. The momentum projection for the matrix element of the pion has the following form,

$$M_{\alpha\beta}^\pi = \frac{if_\pi}{4} \left\{ \not{p} \gamma_5 \Psi_\pi(x, \mathbf{k}_\perp) - m_0^p \gamma_5 \times \left[\Psi_p(x, \mathbf{k}_\perp) - i \sigma_{\mu\nu} \left(n^\mu \bar{n}^\nu \frac{\Psi'_\sigma(x, \mathbf{k}_\perp)}{6} - p^\mu \frac{\Psi_\sigma(x, \mathbf{k}_\perp)}{6} \frac{\partial}{\partial k_{\perp\nu}} \right) \right] \right\}_{\alpha\beta}, \quad (2)$$

where f_π is the pion decay constant and m_0^p is the parameter that can be determined by QCD sum rules [23]. $\Psi_\pi(x, \mathbf{k}_\perp)$ is the leading twist (twist-2) wave function, $\Psi_p(x, \mathbf{k}_\perp)$ and $\Psi_\sigma(x, \mathbf{k}_\perp)$ are subleading twist (twist-3) wave functions, respectively. $\Psi'_\sigma(x, \mathbf{k}_\perp) = \partial \Psi_\sigma(x, \mathbf{k}_\perp) / \partial x$, $n = (\sqrt{2}, 0, \mathbf{0}_\perp)$, and $\bar{n} = (0, \sqrt{2}, \mathbf{0}_\perp)$ are two null vectors that point to the plus and the minus directions, respectively. The momentum projection for the matrix element of the B meson can be written as [12,24]:

$$M_{\alpha\beta}^B = -\frac{if_B}{4} \left\{ \frac{\not{p}_B M_B}{2} \left[\not{p} \Psi_B^+(\xi, \mathbf{1}_\perp) + \not{p} \Psi_B^-(\xi, \mathbf{1}_\perp) - \Delta(\xi, \mathbf{1}_\perp) \gamma^\mu \frac{\partial}{\partial l_\perp^\mu} \right] \gamma_5 \right\}_{\alpha\beta}, \quad (3)$$

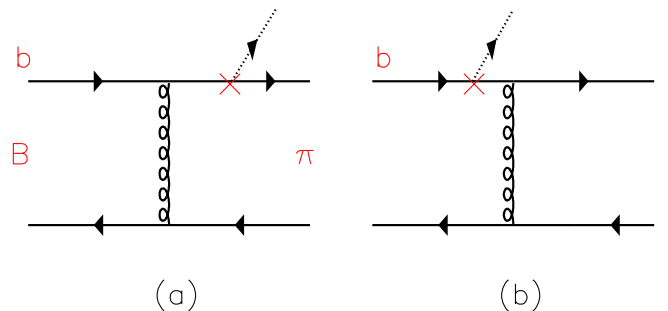


FIG. 1 (color online). Lowest order hard-scattering kernel for $B \rightarrow \pi$ form factor, where the cross denotes an appropriate gamma matrix.

where $\xi = \frac{l^+}{M_B}$ is the momentum fraction for the light spectator quark in the B meson and $\Delta(\xi, \mathbf{1}_\perp) = M_B \int_0^\xi d\xi' [\Psi_B^-(\xi', \mathbf{1}_\perp) - \Psi_B^+(\xi', \mathbf{1}_\perp)]$. Note the four-component l_\perp^μ in Eq. (3) is defined through, $l_\perp^\mu = l^\mu - \frac{(l^+ n^\mu + l^- \bar{n}^\mu)}{2}$ with $l = (\frac{l^+}{\sqrt{2}}, \frac{l^-}{\sqrt{2}}, \mathbf{1}_\perp)$.

In the large recoil regions, the $B \rightarrow \pi$ transition form factor is dominated by a single gluon exchange in the lowest order as depicted in Fig. 1. In the hard-scattering kernel, the transverse momentum in the denominators are retained to regulate the endpoint singularity. The masses of

the light quarks and the mass difference ($\bar{\Lambda}$) between the b quark and the B meson are neglected. The terms proportional to \mathbf{k}_\perp^2 or \mathbf{l}_\perp^2 in the numerator are dropped, which are power suppressed compared to other $\mathcal{O}(M_B^2)$ terms. Under these treatments, the Sudakov form factor from k_T resummation can be introduced into the PQCD factorization theorem without breaking the gauge invariance [21]. In the transverse configuration b -space and by including the Sudakov form factors and the threshold resummation effects, we obtain the formulae for $F_+^{B\pi}(q^2)$ and $F_0^{B\pi}(q^2)$ as following,

$$\begin{aligned}
 F_+^{B\pi}(q^2) = & \frac{\pi C_F}{N_c} f_\pi f_B M_B^2 \int d\xi dx \int b_B db_B b_\pi db_\pi \alpha_s(t) \exp[-S(x, \xi, b_\pi, b_B; t)] S_t(x) S_t(\xi) \\
 & \times \left\{ \Psi_\pi(x, b_\pi) [(x\eta + 1)\Psi_B(\xi, b_B) + (x\eta - 1)\bar{\Psi}_B(\xi, b_B)] + \frac{m_0^p}{M_B} \Psi_p(x, b_\pi) \right. \\
 & \cdot \left[(1 - 2x)\Psi_B(\xi, b_B) + \left(\frac{2}{\eta} - 1\right)\bar{\Psi}_B(\xi, b_B) \right] - \frac{m_0^p}{M_B} \frac{\Psi'_\sigma(x, b_\pi)}{6} \cdot \left[\left(1 + 2x - \frac{2}{\eta}\right)\Psi_B(\xi, b_B) - \bar{\Psi}_B(\xi, b_B) \right] \\
 & + 6 \frac{m_0^p}{M_B} \frac{\Psi_\sigma(x, b_\pi)}{6} \Psi_B(\xi, b_B) \left. \right\} h_1(x, \xi, b_\pi, b_B) - (1 + \eta + x\eta) \frac{m_0^p}{M_B} \frac{\Psi_\sigma(x, b_\pi)}{6} [M_B \Delta(\xi, b_B)] h_2(x, \xi, b_\pi, b_B) \\
 & + \left\{ \Psi_\pi(x, b_\pi) \left(-\xi \bar{\eta} [\Psi_B(\xi, b_B) + \bar{\Psi}_B(\xi, b_B)] + \frac{\Delta(\xi, b_B)}{M_B} \right) + 2 \frac{m_0^p}{M_B} \Psi_p(x, b_\pi) \right. \\
 & \cdot \left. \left[(1 - \xi)\Psi_B(\xi, b_B) + \left(1 + \xi - \frac{2\xi}{\eta}\right)\bar{\Psi}_B(\xi, b_B) + 2 \frac{\Delta(\xi, b_B)}{M_B} \right] \right\} h_1(\xi, x, b_B, b_\pi), \quad (4)
 \end{aligned}$$

and

$$\begin{aligned}
 F_0^{B\pi}(q^2) = & \frac{\pi C_F}{N_c} f_\pi f_B M_B^2 \int d\xi dx \int b_B db_B b_\pi db_\pi \alpha_s(t) \exp[-S(x, \xi, b_\pi, b_B; t)] S_t(x) S_t(\xi) \\
 & \times \left\{ \Psi_\pi(x, b_\pi) \eta [(x\eta + 1)\Psi_B(\xi, b_B) + (x\eta - 1)\bar{\Psi}_B(\xi, b_B)] + \frac{m_0^p}{M_B} \Psi_p(x, b_\pi) \right. \\
 & \times \left[(2 - \eta - 2x\eta)\Psi_B(\xi, b_B) + \eta \bar{\Psi}_B(\xi, b_B) \right] - \frac{m_0^p}{M_B} \frac{\Psi'_\sigma(x, b_\pi)}{6} \\
 & \cdot \left. \left[\eta(2x - 1)\Psi_B(\xi, b_B) - (2 - \eta)\bar{\Psi}_B(\xi, b_B) \right] + 6 \frac{m_0^p}{M_B} \eta \frac{\Psi_\sigma(x, b_\pi)}{6} \Psi_B(\xi, b_B) \right\} \\
 & \times h_1(x, \xi, b_\pi, b_B) - [3 - \eta - x\eta] \frac{m_0^p}{M_B} \frac{\Psi_\sigma(x, b_\pi)}{6} [M_B \Delta(\xi, b_B)] h_2(x, \xi, b_\pi, b_B) \\
 & + \left\{ \Psi_\pi(x, b_\pi) \eta \left(\xi \bar{\eta} [\Psi_B(\xi, b_B) + \bar{\Psi}_B(\xi, b_B)] + \frac{\Delta(\xi, b_B)}{M_B} \right) + 2 \frac{m_0^p}{M_B} \Psi_p(x, b_\pi) \right. \\
 & \cdot \left. \left[\eta(1 + \xi) - 2\xi \right] \Psi_B(\xi, b_B) + \eta(1 - \xi) \bar{\Psi}_B(\xi, b_B) + 2(2 - \eta) \frac{\Delta(\xi, b_B)}{M_B} \right\} h_1(\xi, x, b_B, b_\pi), \quad (5)
 \end{aligned}$$

where

$$\begin{aligned}
 h_1(x, \xi, b_\pi, b_B) = & K_0(\sqrt{\xi x \eta} M_B b_B) [\theta(b_B - b_\pi) \\
 & \times I_0(\sqrt{x \eta} M_B b_\pi) K_0(\sqrt{x \eta} M_B b_B) \\
 & + \theta(b_\pi - b_B) \\
 & \times I_0(\sqrt{x \eta} M_B b_B) K_0(\sqrt{x \eta} M_B b_\pi)], \quad (6)
 \end{aligned}$$

$$\begin{aligned}
 h_2(x, \xi, b_\pi, b_B) = & \frac{b_B}{2\sqrt{\xi x \eta} M_B} K_1(\sqrt{\xi x \eta} M_B b_B) [\theta(b_B - b_\pi) \\
 & \times I_0(\sqrt{x \eta} M_B b_\pi) K_0(\sqrt{x \eta} M_B b_B) \\
 & + \theta(b_\pi - b_B) \\
 & \times I_0(\sqrt{x \eta} M_B b_B) K_0(\sqrt{x \eta} M_B b_\pi)], \quad (7)
 \end{aligned}$$

and we have set,

$$\Psi_B = \frac{\Psi_B^+ + \Psi_B^-}{2}, \quad \bar{\Psi}_B = \frac{\Psi_B^+ - \Psi_B^-}{2}. \quad (8)$$

The functions I_i (K_i) are the modified Bessel functions of the first (second) kind with the i th order. The angular integrations in the transverse plane have been performed. The factor $\exp[-S(x, \xi, b_\pi, b_B; t)]$ contains the Sudakov logarithmic corrections and the renormalization group evolution effects of both the wave functions and the hard-scattering amplitude,

$$S(x, \xi, b_\pi, b_B; t) = \left[s(x, b_\pi, M_b) + s(\bar{x}, b_\pi, M_b) + s(\xi, b_B, M_b) - \frac{1}{\beta_1} \ln \frac{\hat{t}}{\hat{b}_\pi} - \frac{1}{\beta_1} \ln \frac{\hat{t}}{\hat{b}_B} \right], \quad (9)$$

where $\hat{t} = \ln(t/\Lambda_{\text{QCD}})$, $\hat{b}_B = \ln(1/b_B \Lambda_{\text{QCD}})$, $\hat{b}_\pi = \ln(1/b_\pi \Lambda_{\text{QCD}})$, and $s(x, b, Q)$ is the Sudakov exponent factor, whose explicit form up to next-to-leading log approximation can be found in Ref. [15]. $S_t(x)$ and $S_t(\xi)$ come from the threshold resummation effects and here we take a simple parametrization proposed in Refs. [21,25],

$$S_t(x) = \frac{2^{1+2c} \Gamma(3/2 + c)}{\sqrt{\pi} \Gamma(1 + c)} [x(1-x)]^c, \quad (10)$$

where the parameter c is determined to be around 0.3 for the present case.

The hard scale t in $\alpha_s(t)$ and the Sudakov form factor might be varied for the different hard-scattering parts and here we need two t_i [13,21], whose values are chosen as the largest scale of the virtualities of internal particles, i.e.,

$$t_1 = \text{MAX}(\sqrt{x\eta} M_B, 1/b_\pi, 1/b_B), \\ t_2 = \text{MAX}(\sqrt{\xi\eta} M_B, 1/b_\pi, 1/b_B). \quad (11)$$

The Fourier transformation for the transverse part of the wave function is defined as

$$\Psi(x, \mathbf{b}) = \int_{|\mathbf{k}_\perp| < 1/b} d^2 \mathbf{k}_\perp \exp(-i \mathbf{k}_\perp \cdot \mathbf{b}) \Psi(x, \mathbf{k}_\perp), \quad (12)$$

where Ψ stands for Ψ_π , Ψ_p , Ψ_σ , Ψ_B , $\bar{\Psi}_B$, and Δ , respectively. The upper edge of the integration $|\mathbf{k}_\perp| < 1/b$ is necessary to ensure that the wave function is soft enough [26].

In summary, we compare the results in Eqs. (4) and (5) with those in Refs. [12,13,20,21]. In Ref. [20], only leading twist (Ψ_π) of the pion is discussed. Setting the twist-3 terms to zero, the two formulae in Eqs. (4) and (5) and Ref. [20] are in agreement. In Ref. [21], the single B meson wave function Ψ_B is assumed and the terms of $\bar{\Psi}_B$ and Δ are neglected. And in Ref. [13], with a new definition for Ψ_B and $\bar{\Psi}_B$, i.e.,

$$\Psi_B = \Psi_B^+, \quad \bar{\Psi}_B = (\Psi_B^+ - \Psi_B^-), \quad (13)$$

both contributions from Ψ_B and $\bar{\Psi}_B$ are taken into consideration, with only the terms of Δ are neglected. The momentum projector used in [13,21] for the pion is different from the present projector in Eq. (2), i.e., there is no term proportional to Ψ_σ in Refs. [13,21]. Except for these differences¹, the formulae in [13,21] are consistent with ours. Our results agree with Ref. [12], except for several minus errors that should be corrected there.

III. NUMERICAL CALCULATIONS

In the numerical calculations, we use

$$\Lambda_{\overline{MS}}^{(n_f=4)} = 250 \text{ MeV}, \quad f_\pi = 131 \text{ MeV}, \\ f_B = 190 \text{ MeV}, \quad m_0^p = 1.30 \text{ GeV}. \quad (14)$$

The wave functions in the compact parameter b -space, $\Psi_+^B(\xi, b_B)$, $\Psi_-^B(\xi, b_B)$, $\Psi_\pi(x, b_\pi)$, $\Psi_p(x, b_\pi)$, and $\Psi_\sigma(x, b_\pi)$ can be found in the appendix. The k_T -dependence has been kept in both the B meson and the pion wave functions. As has been argued in several papers [22,27–29], the intrinsic k_T -dependence of the wave function is important and the results will be overestimated without including this effect, so it is necessary to include the transverse momentum dependence into the wave functions not only for the B meson but also for the pion. As has been argued in Ref. [22], we take $m_0^p = 1.30 \text{ GeV}$ for latter discussions, which is a little below the value given by the chiral perturbation theory [30].

The two wave functions Ψ_B and $\bar{\Psi}_B$ of the B meson shown in the appendix depend only on the effective mass ($\bar{\Lambda} = M_B - m_b$) of the B meson. An estimate of $\bar{\Lambda}$ using QCD sum rule approach gives $\bar{\Lambda} = 0.57 \pm 0.07 \text{ GeV}$ [31]. In Fig. 2, we show the $B \rightarrow \pi$ transition form factor with a different value of $\bar{\Lambda}$, where the shaded band is drawn with a broader range for $\bar{\Lambda}$, i.e., $\bar{\Lambda} \in (0.4 \text{ GeV}, 0.7 \text{ GeV})$. And for comparison, we show the QCD LCSR result [5] in a solid line and its theoretical error ($\pm 10\%$) by a fuscous shaded band in Fig. 2. The results show that the $B \rightarrow \pi$ transition form factor will decrease with the increment of $\bar{\Lambda}$. When $\bar{\Lambda} \in (0.5 \text{ GeV}, 0.6 \text{ GeV})$, one may observe that the present results agree well with the QCD LCSR results [4,5] up to $q^2 \sim 14 \text{ GeV}^2$. In Fig. 2, for simplicity, only the QCD LCSR results of Ref. [5] are shown. The LCSR results in Refs. [4,5] are in agreement with each other even though they have taken different ways to improve the QCD LCSR calculation precision, i.e., in Ref. [4], an alternative way to do the QCD LCSR calculation is adopted in which the pionic twist-3 contributions are avoided by calculating the correlator with a proper chiral current and then the leading twist contributions are calcu-

¹According to the power counting rules in Ref. [21], the terms that do not exist in Ref. [21] are defined as subleading terms in $1/M_B$ and are neglected accordingly. And here, we keep all the terms with care.

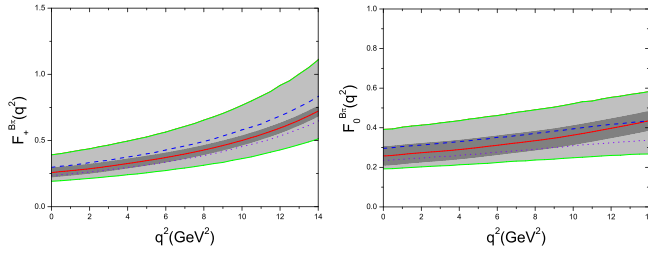


FIG. 2 (color online). PQCD results for the $B \rightarrow \pi$ transition form factors $F_+^{B\pi}(q^2)$ (Left) and $F_0^{B\pi}(q^2)$ (Right) with different values for $\bar{\Lambda}$. The dashed line stands for $\bar{\Lambda} = 0.5$ GeV, the dotted line stands for $\bar{\Lambda} = 0.6$ GeV, the upper edge of the shaded band corresponds to $\bar{\Lambda} = 0.40$ GeV, and the lower edge of the band corresponds to $\bar{\Lambda} = 0.70$ GeV. For comparison, the solid line comes from the QCD LCSR [4,5] and the fuscous shaded band shows its theoretical error $\pm 10\%$.

lated up to next-to-leading order; while in Ref. [5], the usual QCD LCSR approach is adopted and both the twist-2 and twist-3 contributions are calculated up to next-to-leading order. In Ref. [13], $\bar{\Lambda}$ is treated as a free parameter and a bigger value is adopted there, i.e., $\bar{\Lambda} = (0.70 \pm 0.05)$ GeV. The main reason is that in the present paper, we have used an improved form (with better endpoint behavior than that of the asymptotic one) for the pionic twist-3 wave function Ψ_p , while in Ref. [13], they took ϕ_p in Ref. [7] (with an endpoint behavior even worse than the asymptotic one) other than Ψ_p to do the calculations, so the value of $\bar{\Lambda}$ in Ref. [13] must be big enough to suppress the endpoint singularity coming from the hard kernel. For clarity, if not specifically stated, we shall fix $\bar{\Lambda}$ to be 0.5 GeV in the following discussions.

Second, to get a deep understanding of the $B \rightarrow \pi$ transition form factor, we discuss the contributions from different parts of the B meson wave function or the pion wave function, correspondingly. Here we take $F_+^{B\pi}(q^2)$ to do our discussions and the case of $F_0^{B\pi}(q^2)$ can be done in a similar way. In Fig. 3(a), we show the contributions from the different twist structures of the pion wave function, i.e.,

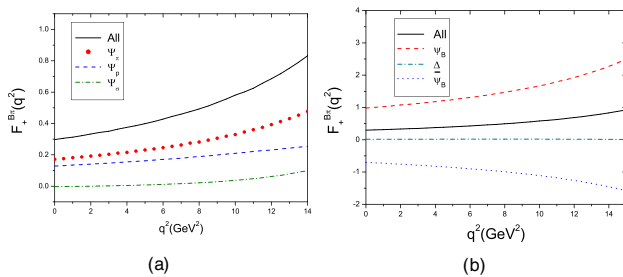


FIG. 3 (color online). PQCD results for the $B \rightarrow \pi$ transition form factor $F_+^{B\pi}(q^2)$ with fixed $\bar{\Lambda} = 0.5$ GeV. The left diagram is for the different pion twist structures, Ψ_π , Ψ_p , and Ψ_σ . The right diagram is for the different B meson structures, Ψ_B , $\bar{\Psi}_B$, and Δ , where Ψ_B and $\bar{\Psi}_B$ are defined in Eq. (8).

Ψ_π , Ψ_p , and Ψ_σ (the contributions from the terms involving Ψ'_σ are included in Ψ_σ), respectively. From Fig. 3(a), one may observe that the contribution from Ψ_π is the biggest, then comes that of Ψ_p and Ψ_σ . And the ratio between all the twist-3 contributions and the leading twist contribution is $\sim 70\%$ in the large recoil regions. This behavior is quite different from the conclusion that has been drawn in Refs. [12,21], in which they concluded that the twist-3 contribution is bigger than that of the twist-2 contribution, especially in Ref. [12], where it claimed that the twist-3 contribution is about 3 times bigger than that of twist-2 at $q^2 = 0$. Such kinds of big twist-3 contributions are due to the fact that they only took the pion distribution amplitudes into consideration (or simply adding a harmonic transverse momentum dependence for the pion wave functions), and then the endpoint singularity coming from the hard kernel cannot be effectively suppressed, especially for Ψ_p whose DA's asymptotic behavior is $\phi_p \equiv 1$. In Ref. [22], the authors have made a detailed analysis on the model dependence of the twist-3 contributions to the pion electromagnetic form factor, and have raised a new twist-3 wave function (as is shown in the appendix) with a better endpoint behavior for Ψ_p , which is inspired from QCD sum rule moment calculation. With this model wave function for Ψ_p , Ref. [22] shows that the twist-3 contributions of the pion electromagnetic form factor agree well with the power counting rule, i.e., the twist-3 contribution drops fast and it becomes less than the twist-2 contribution at $Q^2 \sim 10$ GeV². For the present B meson case, according to the power counting rules in Ref. [21], the twist-3 contribution and the twist-2 contribution are of the same order, however one may find from Fig. 3(a) that with a new form with better endpoint behavior for Ψ_p , the twist-3 contribution can be effectively suppressed and then its contribution is less than the leading twist contribution.

Now we show to what extent $\bar{\Psi}_B$ will affect the final results. Figure 3(b) presents the contributions from Ψ_B , $\bar{\Psi}_B$, and Δ respectively, where Ψ_B and $\bar{\Psi}_B$ are defined in Eq. (8). From Fig. 3(b), one may observe that the contribution from Δ is quite small and can be safely neglected as has been done in most of the calculations. However the contribution from $\bar{\Psi}_B$ is quite large, i.e., at $q^2 = 0$, the ratio between the contributions of $\bar{\Psi}_B$ and Ψ_B is about (-70%) , which roughly agrees with the observation in Ref. [12]. So the negative contribution from $\bar{\Psi}_B$ cannot be neglected, and it is necessary to suppress the big positive contribution from Ψ_B so as to get a more reasonable total contributions from both Ψ_B and $\bar{\Psi}_B$. The above results of Fig. 3(b) are obtained by using the definition Eq. (8). A new definition (13) for Ψ_B and $\bar{\Psi}_B$ has been raised in Ref. [13] and the contributions from the Ψ_B , $\bar{\Psi}_B$, and Δ with such a new definition (13) are shown in Fig. 4(a). We draw the distribution of the corresponding

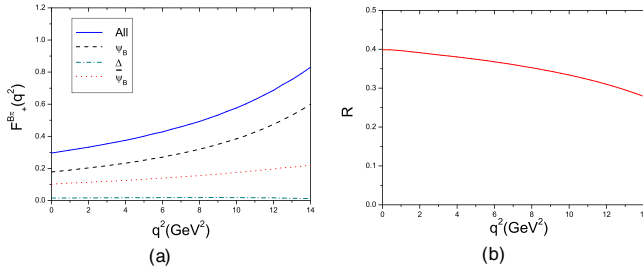


FIG. 4 (color online). PQCD results for the $B \rightarrow \pi$ form factor $F_+^{B\pi}(q^2)$ with fixed $\bar{\Lambda} = 0.5$ GeV, where Ψ_B and $\bar{\Psi}_B$ are defined in Eq. (13). The left diagram shows the contributions from different B meson wave functions, Ψ_B , $\bar{\Psi}_B$, and Δ , respectively. The right diagram is the distribution of the ratio $R = \left(\frac{F_+^{B\pi}|_{\bar{\Psi}_B}}{F_+^{B\pi}|_{\text{All}}}\right)$ versus q^2 .

ratio $R = \left(\frac{F_+^{B\pi}|_{\bar{\Psi}_B}}{F_+^{B\pi}|_{\text{All}}}\right)$ versus q^2 in Fig. 4(b), where $(F_+^{B\pi}|_{\bar{\Psi}_B})$ means that only the contributions from $\bar{\Psi}_B$ are considered and $(F_+^{B\pi}|_{\text{All}})$ means that all the contributions from the B meson wave functions are taken into consideration. One may observe from Fig. 4(b) that even with the new definition (13) for Ψ_B and $\bar{\Psi}_B$, the contribution from $\bar{\Psi}_B$ is not small ($\sim 25\%$ – 40%) and it cannot be safely neglected. Thus both Ψ_B and $\bar{\Psi}_B$ should be kept in the calculation for giving a better understanding of the B decays.

Finally, we make a comparison of the present results for $F_{+,0}^{B\pi}(q^2)$ with those obtained in Ref. [21] in Fig. 5. In Ref. [21], $\bar{\Psi}_B$ has been neglected and Ψ_B takes the form

$$\Psi_B(x, b_B) = N_B x^2 (1-x)^2 \exp\left[-\frac{1}{2}\left(\frac{xM_B}{\omega_B}\right)^2 - \frac{\omega_B^2 b_B^2}{2}\right], \quad (15)$$

where N_B is the normalization factor and ω_B is taken to be (0.40 ± 0.04) GeV. In Fig. 5, we show their results for $\omega_B = 0.36$ GeV, 0.40 GeV, and 0.44 GeV and our present results with $\bar{\Lambda} \in (0.5$ GeV, 0.6 GeV), respectively. The

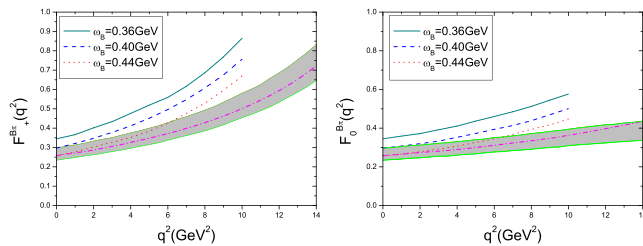


FIG. 5 (color online). Comparison of different PQCD results for the $B \rightarrow \pi$ transition form factors $F_+^{B\pi}(q^2)$ (Left) and $F_0^{B\pi}(q^2)$ (Right). The solid, dashed and dotted lines are the results obtained in Ref. [21] and are for $\omega_B = 0.36$ GeV, 0.40 GeV, and 0.44 GeV, respectively. The shaded band are our present results with the upper edge for $\bar{\Lambda} = 0.50$ GeV and the lower edge for $\bar{\Lambda} = 0.60$ GeV, respectively. For comparison, the dash-dot line stands for the QCD LCSR result [4,5].

two results in the large recoil regions $q^2 \sim 0$ are consistent with each other, however one may observe that the fast rise in Ref. [21] has been suppressed in our present results and the slope of the present obtained form factors $F_{+,0}^{B\pi}(q^2)$ are more consistent with the QCD LCSR results in Refs. [4,5]. The main reason for the differences between our present results and those in Ref. [21] is that we have used a better endpoint behavior wave function for Ψ_p [22]. With this new form for Ψ_p , we find that the total twist-3 contributions are in fact less than ($\sim 70\%$) the leading twist contribution in the large recoil regions. Whereas in Ref. [21], the twist-3 contributions are about 2 times bigger than that of the leading twist, especially for the bigger q^2 regions, and then the total contributions will give a fast rise in shape.

IV. DISCUSSION AND SUMMARY

In the present paper, we have examined the $B \rightarrow \pi$ transition form factor in the PQCD approach, where the transverse momentum dependence for the wave function, the Sudakov effects, and the threshold effects are included to regulate the endpoint singularity and to derive a more reasonable result. We emphasize that the transverse momentum dependence for both the B meson and the pion is important to give a better understanding of the $B \rightarrow \pi$ transition form factor. The pionic twist-3 contributions to the $B \rightarrow \pi$ transition form factor are carefully studied with a better endpoint behavior wave function for Ψ_p , and Fig. 3 shows that the twist-3 contributions are of the same order of the leading twist contribution, however its values are less than that of the leading twist. This observation improves the results obtained in Refs. [12,21], in which the asymptotic behavior for ϕ_p was used and they claimed a large twist-3 contributions to the $B \rightarrow \pi$ transition form factor, i.e., bigger than that of the leading twist. Figures 3(b) and 4 show that both Ψ_B and $\bar{\Psi}_B$ are important, no matter what definition [Eq. (8) or Eq. (13)] is chosen. Under the definition (8), the negative contribution from $\bar{\Psi}_B$ is necessary to suppress the big contribution from Ψ_B and to obtain a reasonable number of total contributions. While under the definition Eq. (13), the contribution from $\bar{\Psi}_B$ is power suppressed to that of Ψ_B , however it still can contribute 25% – 40% to the total contributions. As is shown in Fig. 5, a comparison of our present results for $F_{+,0}^{B\pi}(q^2)$ with those in Ref. [21] shows that a better PQCD result (with its slope closest to the QCD LCSR results) can be obtained by carefully considering both the pionic twist-3 contributions and the contributions from the two wave functions Ψ_B and $\bar{\Psi}_B$ of the B meson.

In the literature, the values of the $B \rightarrow \pi$ transition form factors $F_+^{B\pi}(0)$ and $F_0^{B\pi}(0)$ are determined to be around 0.3 . With $\bar{\Lambda} \in (0.50$ GeV, 0.60 GeV), we obtain $F_{+,0}^{B\pi}(0) = 0.265 \pm 0.032$. This result is consistent with the extrapolated lattice QCD result $F_{+,0}^{B\pi}(0) = 0.27 \pm 0.11$ [1] and the

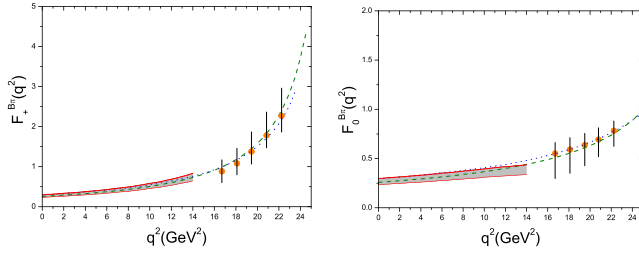


FIG. 6 (color online). PQCD results for the $B \rightarrow \pi$ form factors $F_+^{B\pi}(q^2)$ (Left) and $F_0^{B\pi}(q^2)$ (Right). The shaded band represents our present results with the upper edge for $\bar{\Lambda} = 0.50$ GeV and the lower edge for $\bar{\Lambda} = 0.60$ GeV, respectively. The dashed lines and dotted lines stand for the QCD LCSR result Eq. (16) and the fits to the lattice QCD results with errors [3], respectively.

newly obtained QCD LCSR result $F_{+,0}^{B\pi}(0) = 0.258 \pm 0.031$ [5]. The PQCD calculation are reliable only when the involved energy scale is hard enough. The lattice QCD calculations which presently are available only for the soft regions, i.e. $q^2 > 15$ GeV². The QCD LCSR can treat both hard and soft contributions with $q^2 \leq 18$ GeV² [4,5] on the same footing. Therefore, the results from the PQCD approach, the lattice QCD approach, and the QCD LCSRs are complementary to each other and by combining the results of those three approaches, one may obtain an understanding of the $B \rightarrow \pi$ transition form factor in the whole physical regions. The $B \rightarrow \pi$ transition form factors $F_+^{B\pi}(q^2)$ and $F_0^{B\pi}(q^2)$ derived from QCD LCSRs can be written in the following parametrization [5]:

$$\begin{aligned} F_+^{B\pi}(q^2) &= \frac{r_1}{1 - q^2/m_1^2} + \frac{r_2}{1 - q^2/m_{\text{fit}}^2}, \\ F_0^{B\pi}(q^2) &= \frac{r_3}{1 - q^2/m_{0\text{fit}}^2}, \end{aligned} \quad (16)$$

where $r_1, r_2, r_3, m_1, m_{\text{fit}}$, and $m_{0\text{fit}}$ are fitted parameters and can be taken as [5], $r_1 = 0.744, r_2 = -0.486, r_3 = 0.258, m_1 = 5.32$ GeV, $m_{\text{fit}}^2 = 40.73$ GeV², and $m_{0\text{fit}}^2 = 33.81$ GeV². With the parametrization Eq. (16), the QCD LCSR results can be extrapolated up to the upper limit of q^2 , i.e., $q^2 \sim 25$ GeV², and then it can be treated as a bridge to connect both the PQCD results and the lattice QCD results. In Fig. 6, we show the results of the PQCD approach, the lattice QCD approach and the extrapolated QCD LCSR results defined in Eq. (16), respectively. Our present PQCD results with $\bar{\Lambda} \in (0.5 \text{ GeV}, 0.6 \text{ GeV})$ are in agreement and can match with the QCD LCSR results and the lattice QCD calculations, which are shown in Fig. 6.

In summary, we have shown that the PQCD approach can be applied to calculate the $B \rightarrow \pi$ transition form factor in the large recoil regions. The twist-3 contributions obtained by using better endpoint behavior twist-3 wave functions are less than the leading twist contributions and both of the two wave functions Ψ_B and $\bar{\Psi}_B$ of the B meson

are necessary to give a deep understanding of the B decays, e.g., the $B \rightarrow \pi$ transition form factor. Combining the PQCD results with the QCD LCSR and the lattice QCD calculations, the $B \rightarrow \pi$ transition form factor can be determined in the whole kinematic regions.

ACKNOWLEDGMENTS

The authors would like to thank H. N. Li for some useful discussions. This work was supported in part by the Natural Science Foundation of China (NSFC).

APPENDIX: FORMULAE FOR THE PION AND B MESON WAVE FUNCTIONS

To do the numerical calculations for the pion wave functions, we take

$$\Psi_{\pi,\sigma}(x, \mathbf{k}_\perp) = A_\pi \exp\left(-\frac{m^2 + k_\perp^2}{8\beta^2 x(1-x)}\right), \quad (A1)$$

where the parameters can be determined by the normalization condition of the wave function

$$\int_0^1 dx \int \frac{d^2\mathbf{k}_\perp}{16\pi^3} \Psi(x, \mathbf{k}_\perp) = 1, \quad (A2)$$

and some necessary constraints [32]. One can construct a model wave function Ψ_p with k_T dependence in the following [22],

$$\begin{aligned} \Psi_p(x, \mathbf{k}_\perp) &= [1 + B_p C_2^{1/2}(1-2x) + C_p C_4^{1/2}(1-2x)] \\ &\times \frac{A_p}{x(1-x)} \exp\left(-\frac{m^2 + k_\perp^2}{8\beta^2 x(1-x)}\right), \end{aligned} \quad (A3)$$

where $C_2^{1/2}(1-2x)$ and $C_4^{1/2}(1-2x)$ are Gegenbauer polynomials and the coefficients A_p, B_p , and C_p can be determined by the DA moments. In the above equations

$$m = 290 \text{ MeV}, \quad \beta = 385 \text{ MeV}, \quad (A4)$$

which are derived for $\langle \mathbf{k}_\perp^2 \rangle \approx (356 \text{ MeV})^2$ [32]. The parameters in Eq. (A3) can then be determined as,

$$\begin{aligned} A_\pi &= 1.187 \times 10^{-3} \text{ MeV}^{-2}, \quad A_p = 2.841 \times 10^{-4} \text{ MeV}^{-2}, \\ B_p &= 1.302, \quad C_p = 0.126. \end{aligned} \quad (A5)$$

For the B meson wave function, we take [19,33]

$$\begin{aligned} \Psi_B^-(\xi, \mathbf{k}_\perp) &= 16\pi^3 \frac{2\bar{\xi} - \xi}{2\pi\bar{\xi}^2} \theta(2\bar{\xi} - \xi) \\ &\times \delta[k_\perp^2 - M_B^2 \xi(2\bar{\xi} - \xi)], \end{aligned} \quad (A6)$$

$$\begin{aligned} \Psi_B^+(\xi, \mathbf{k}_\perp) &= 16\pi^3 \frac{\xi}{2\pi\bar{\xi}^2} \theta(2\bar{\xi} - \xi) \\ &\times \delta[k_\perp^2 - M_B^2 \xi(2\bar{\xi} - \xi)], \end{aligned} \quad (A7)$$

with $\xi = \frac{t^+}{M_B}$ and $\bar{\xi} = \frac{\bar{t}}{M_B}$, where $\bar{\Lambda}$ is the effective mass of the B meson.

After doing the Fourier transformation with the formula Eq. (12), we obtain

$$\Psi_{\pi,\sigma}(x, b_\pi) = 2\pi A_\pi \int_0^{1/b_\pi} \exp\left(-\frac{m^2}{8\beta^2 x(1-x)}\right) J_0(b_\pi k_\perp) k_\perp dk_\perp \quad (\text{A8})$$

$$\Psi_p(x, b_p) = \frac{2\pi A_p}{x(1-x)} [1 + B_p C_2^{1/2}(1-2x) + C_p C_4^{1/2}(1-2x)] \cdot \int_0^{1/b_p} \exp\left(-\frac{m^2}{8\beta^2 x(1-x)}\right) J_0(b_p k_\perp) k_\perp dk_\perp \quad (\text{A9})$$

$$\Psi_B^-(\xi, b_B) = 16\pi^3 \frac{2\bar{\xi} - \xi}{2\bar{\xi}^2} \theta(2\bar{\xi} - \xi) \times \theta[1/b_B^2 - \xi(2\bar{\xi} - \xi)M_B^2] \times J_0\left(M_B b_B \sqrt{\xi(2\bar{\xi} - \xi)}\right) \quad (\text{A10})$$

$$\Psi_B^+(\xi, b_B) = 16\pi^3 \frac{\xi}{2\bar{\xi}^2} \theta(2\bar{\xi} - \xi) \theta[1/b_B^2 - \xi(2\bar{\xi} - \xi)M_B^2] J_0\left(M_B b_B \sqrt{\xi(2\bar{\xi} - \xi)}\right) \quad (\text{A11})$$

$$\Delta(\xi, b_B) = M_B \int_0^\xi d\xi' [\Psi_B^-(\xi', b_B) - \Psi_B^+(\xi', b_B)] = 16\pi^3 M_B \theta[1/b_B^2 - \xi(2\bar{\xi} - \xi)M_B^2] \times \int_0^\xi \frac{\bar{\xi} - \xi'}{\bar{\xi}^2} J_0\left(M_B b_B \sqrt{\xi'(2\bar{\xi} - \xi')}\right) d\xi'. \quad (\text{A12})$$

One may easily find that the effects of the upper limit ($1/b_B$) for the B meson wave functions are quite small (numerically less than 0.1%). This is reasonable, since the B meson mass is heavy enough to give a natural separation scale.

-
- [1] L. D. Debbio, J. M. Flynn, L. Lellouch, and J. Nieves, Phys. Lett. B **416**, 392 (1998).
[2] D. Becirevic, Nucl. Phys. B, Proc. Suppl. **94**, 337 (2001).
[3] K. C. Bowler, *et al.*, Phys. Lett. B **486**, 111 (2000).
[4] T. Huang, Z. H. Li, and X. Y. Wu, Phys. Rev. D **63**, 094001 (2001); Z. G. Wang, M. Z. Zhou, and T. Huang, Phys. Rev. D **67**, 094006 (2003).
[5] P. Ball and R. Zwicky, Phys. Rev. D **71**, 014015 (2005).
[6] A. Khodjamirian, R. Ruckl, S. Weinzierl, C. W. Winhart, and O. Yakovlev, Phys. Rev. D **62**, 114002 (2000).
[7] P. Ball, J. High Energy Phys. **09** (1998) 005.
[8] M. Wirbel, B. Stech, and M. Bauer, Z. Phys. C **29**, 637 (1985).
[9] H. N. Li, Phys. Rev. D **52**, 3958 (1995); H. N. Li and B. Melic, Eur. Phys. J. C **11**, 695 (1999); C. D. Lu, K. Ukai, and M. Z. Yang, Phys. Rev. D **63**, 074009 (2001); M. Dahm, R. Jacob, and P. Kroll, Z. Phys. C **68**, 595 (1995).
[10] A. Szczepaniak, E. M. Henley, and S. J. Brodsky, Phys. Lett. B **243**, 287 (1990); S. J. Brodsky, Report No. SLAC-PUB-5529 (unpublished); S. J. Brodsky, Report No. SLAC-PUB-5917 (unpublished).
[11] Y. Y. Keum, H. N. Li, and A. I. Sanda, Phys. Rev. D **63**, 054008 (2001).
[12] Z. T. Wei and M. Z. Yang, Nucl. Phys. **B642**, 263 (2002).
[13] C. D. Lu and M. Z. Yang, Eur. Phys. J. C **28**, 515 (2003).
[14] Chia-Hung V. Chang and H. N. Li, Phys. Rev. D **55**, 5577 (1997); T. W. Yeh and H. N. Li, Phys. Rev. D **56**, 1615 (1997); M. Nagashima and H. N. Li, Phys. Rev. D **67**, 034001 (2003).
[15] H. N. Li and H. L. Yu, Phys. Rev. Lett. **74**, 4388 (1995); Phys. Lett. B **353**, 301 (1995); Phys. Rev. D **53**, 2480 (1996).
[16] G. P. Lepage and S. J. Brodsky, Phys. Rev. Lett. **43**, 545 (1979); **43**, 1625(E) (1979); G. P. Lepage and S. J. Brodsky, Phys. Lett. **87B**, 359 (1979); G. P. Lepage and S. J. Brodsky, Phys. Rev. D **22**, 2157 (1980); A. V. Efremov and A. V. Radyushkin, Phys. Lett. **94B**, 245 (1980); H. N. Li and G. Sterman, Nucl. Phys. **B381**, 129 (1992).
[17] T. Huang and C. W. Luo, Commun. Theor. Phys. **22**, 473 (1994); A. Khodjamirian, R. Ruckl, and C. W. Winhart, Phys. Rev. D **58**, 054013 (1998).
[18] G. Sterman, Phys. Lett. B **179**, 281 (1986); Nucl. Phys. **B281**, 310 (1987); S. Catani and L. Trentadue, Nucl. Phys. **B327**, 323 (1989); **B353**, 183 (1991).
[19] T. Huang, X. G. Wu, and M. Z. Zhou, hep-ph/0412225.
[20] S. D. Genon and C. T. Sachrajda, Nucl. Phys. **B625**, 239 (2002).
[21] T. Kurimoto, H. N. Li, and A. I. Sanda, Phys. Rev. D **65**, 014007 (2002).
[22] T. Huang and X. G. Wu, Phys. Rev. D **70**, 093013 (2004).

- [23] T. Huang, X.H. Wu, and M.Z. Zhou, Phys. Rev. D **70**, 014013 (2004).
- [24] M. Beneke and T. Feldmann, Nucl. Phys. **B592**, 3 (2001).
- [25] H.N. Li, Phys. Rev. D **66**, 094010 (2002).
- [26] J. Botts and G. Sterman, Nucl. Phys. **B325**, 62 (1989); F.G. Cao and T. Huang, Mod. Phys. Lett. A **13**, 253 (1998).
- [27] T. Huang, X.G. Wu, and X.H. Wu, Phys. Rev. D **70**, 053007 (2004).
- [28] R. Jacob and P. Kroll, Phys. Lett. B **315**, 463 (1993); **319**, 545(E) (1993); L.S. Kisslinger and S.W. Wang, hep-ph/9403261.
- [29] Z.T. Wei and M.Z. Yang, Phys. Rev. D **67**, 094013 (2003).
- [30] A. Pich, hep-ph/9806303; P. Ball, J. High Energy Phys. 01 (1999) 010.
- [31] M. Neubert, Phys. Rep. **245**, 259 (1994).
- [32] T. Huang, B.Q. Ma, and Q.X. Shen, Phys. Rev. D **49**, 1490 (1994).
- [33] H. Kawamura, J. Kodaira, C.F. Qiao, and K. Tanaka, Phys. Lett. B **523**, 111 (2001); **536**, 344(E) (2002); Nucl. Phys. B, Proc. Suppl. **116**, 269 (2003); Mod. Phys. Lett. A **18**, 799 (2003).